

**UNCLASSIFIED**

**AD 419034**

**DEFENSE DOCUMENTATION CENTER**

**FOR**

**SCIENTIFIC AND TECHNICAL INFORMATION**

**CAMERON STATION, ALEXANDRIA, VIRGINIA**



**UNCLASSIFIED**

NOTICE: When government or other drawings, specifications or other data are used for any purpose other than in connection with a definitely related government procurement operation, the U. S. Government thereby incurs no responsibility, nor any obligation whatsoever; and the fact that the Government may have formulated, furnished, or in any way supplied the said drawings, specifications, or other data is not to be regarded by implication or otherwise as in any manner licensing the holder or any other person or corporation, or conveying any rights or permission to manufacture, use or sell any patented invention that may in any way be related thereto.

419034

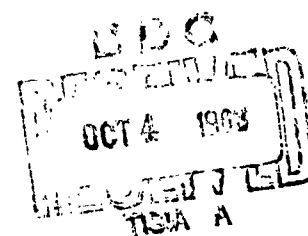
CATALOGED BY DDC<sup>179</sup>  
AS AD No. 419034

64-5  
CONTRACT NO. NONR 839(14)  
PROJECT NO. NR 064-167

PRESSURIZED RING-REINFORCED OVAL CYLINDER  
- COMPARISON OF THEORY AND DTMB TESTS

by

Joseph Kempner, William P. Vafakos and Neil Nissel



POLYTECHNIC INSTITUTE OF BROOKLYN

DEPARTMENT  
of  
AEROSPACE ENGINEERING  
and  
APPLIED MECHANICS

SEPTEMBER 1963

PIBAL REPORT NO. 671

Contract No. Nonr 839(14)  
Project No. NR 064-167

**PRESSURIZED RING-REINFORCED OVAL CYLINDER  
- COMPARISON OF THEORY AND DTMB TESTS**

by

**Joseph Kempner, William P. Vafakos and Neil Nissel**

**Polytechnic Institute of Brooklyn**

**Department of  
Aerospace Engineering and Applied Mechanics**

**September 1963**

**PIBAL Report No. 671**

**Reproduction in whole or in part is permitted for any purpose  
of the United States Government.**

## SUMMARY

Theoretical results for the stresses occurring in a ring-reinforced oval cylindrical shell subjected to a hydrostatic pressure are compared with corresponding test results recently published by the David Taylor Model Basin. The cylinder treated is composed of two different skin thicknesses. The theoretical results are obtained by using the local skin thickness of the cylinder in solutions developed for ring-reinforced short oval cylinders of uniform thickness. Good agreement is shown to exist between the results of theory and test for all circumferential stresses and for the axial bending stresses, but not for the axial membrane stresses. It is indicated that the solution based upon using the local skin thickness can not be expected to yield accurate results for these latter stresses. However, these can be shifted towards the test results by applying a simple one-dimensional correction.

## INTRODUCTION

In order to provide structural designers and analysts with a better understanding of the behavior of ring-reinforced oval cylindrical shells subjected to hydrostatic pressure, a subject about which little appears in the literature, the David Taylor Model Basin has published the results of recent model tests (Ref. 1). This note presents, for comparison, theoretical results for the ring-stiffened oval cylinder reported upon in Ref. 1. The theoretical results have been obtained by extending to a ring-reinforced oval cylinder an energy solution for short oval shells which has previously been successfully applied to both clamped (Ref. 2) and simply supported (Ref. 3) oval shells.

# PROCEDURE FOR SOLUTION

In Ref. 2 an eight function energy solution, which is applicable to arbitrary edge conditions, is developed for short oval cylindrical shells of uniform skin thickness  $h$ . In that solution it is assumed that  $h \ll r$  and that the local curvature  $1/r$  of the median line of the oval cross section is given by

$$1/r = (1/r_0)[1 + \xi \cos(4\pi s/L_0)] \quad (1)$$

where  $\xi$  is an eccentricity parameter which fixes the major-to-minor axis ratio  $b/a$ ,  $L_0$  is the length of the oval cross section,  $r_0 = L_0/2\pi$  is the mean radius, and  $s$  is a circumferential coordinate measured from an end of the major axis ( $0 \leq s \leq L_0$ ).

By applying the theorem of the minimum of the total potential the eight functions (of the axial coordinate  $x$ ) are determined. The corresponding solution contains enough constants of integration to satisfy arbitrary edge conditions. The theoretical results of this note were obtained by determining the constants so as to satisfy the boundary conditions for a typical bay of a periodically ring-stiffened oval cylinder. This analysis included the determination of expressions for the displacements and stresses in the oval ring, which is subjected to the interaction

load between the ring and shell. The details of such ring calculations in which deep ring equations are used will be reported upon separately.

As is shown in Fig. 1, the cross section of the model tested by the David Taylor Model Basin is composed of two constant radii and two different skin thicknesses, i.e., the cross section is not of the form of Eq. 1 nor is  $h$  a constant. Neither of these geometric properties are consistent with the theory used. The fact that the model cross section does not conform to Eq. 1 does not pose any real difficulty in analysis, since the model can be very closely approximated by an appropriate choice of the parameters in Eq. 1. These were chosen so that both the model tested and its theoretical counterpart had the same values of  $L_0 = 84.44"$  and  $b/a \approx 1.5$ . These quantities were obtained by using  $r_0 = 13.44"$  and  $\xi = 0.61$ , which imply that the major and minor axes are  $b = 31.60"$  and  $a = 20.80"$ , respectively. These values compare favorably with those consistent with Fig. 1, i.e.,  $b = 31.615"$  and  $a = 20.981"$ .

However, a major difficulty in applying the shell solution of Ref. 2 to the model of Fig. 1 does arise since that model is composed of two different skin thicknesses, whereas the solution is applicable only to a shell of uniform thickness. To circumvent this difficulty, the following artifice was used.



The solution for the model of Fig. 1 was assumed to be adequately approximated by using the local thicknesses of that model in the eight function solution developed in Ref. 2 for a shell of uniform thickness, i.e., the solution was obtained for each of two different theoretical models. Both models were assumed to have cross-sectional dimensions (discussed above), axial bay length  $L$  and reinforcing rings corresponding to Fig. 1. However, different uniform skin thicknesses were assumed for each model. These corresponded to the two different skin thicknesses of the model tested, i.e.,  $h = h_1 = 0.385"$  and  $h = h_2 = 0.211"$ . The solution for a quadrant of the reinforced cylinder of Fig. 1 was assumed to be given by the solution for  $h = h_2$  in the range  $0 \text{ (major axis)} \leq s \leq 9.42"$  (point of tangency) and by the solution for  $h = h_1$  in the range  $9.42 \leq s \leq 21.11"$  (minor axis).

## DISCUSSION

The experimental points and the dashed curves (local radius of curvature solution) for the nondimensional stress  $\sigma = (\text{dimensional stress/hydrostatic pressure})$  shown in Figs. 2 through 8 have been taken from Ref. 1. In these figures  $\sigma_x$  and  $\sigma_\theta$ , respectively, are the nondimensional axial and circumferential stresses, and the location of the weld corresponds to the point of tangency in Fig. 1. Local radius of curvature solutions, in which solutions for oval cylinders are obtained by using the local radius of curvature of the oval in the corresponding solution for a circular cylinder, have been shown in Refs. 2 and 3 to yield good results for clamped and simply supported short oval cylinders. However, as has been conjectured in Ref. 2 and shown in Ref. 1, this type of approximate solution does not yield good results for the case of ring-reinforced oval cylinders. All solid lines in the figures are the result of using the local thickness of the ring-reinforced oval cylinder in the solution obtained for a shell of uniform thickness, as has been discussed in the section above.

Figs. 2 and 3, respectively, are plots of  $\sigma_x$  and  $\sigma_\theta$  versus  $x$  for the inside and outside surfaces of the shell at the major axis. Figs. 4 and 5 are corresponding plots at the minor

axis, whereas Figs. 6 and 7 show these stresses for a quadrant of the shell at mid-bay. The abscissa  $\theta$  in these latter figures is the angle which a normal to the median surface of the shell in Fig. 1 makes with the major axis. The junction of the two different shell thicknesses, i.e., the weld, occurs at  $\theta = 62.1^\circ$ . In Fig. 8 plots are shown for the circumferential flange stresses in the ring. These theoretical and experimental ring stresses are seen to be in particularly good agreement.

The solid curves in Figs. 2 through 8, which are based upon the eight function energy solution in which the local shell thickness has been used, show remarkable agreement between theory and test for the stresses  $\sigma_\theta$ . In many instances these curves pass right through the test data. On the other hand, the corresponding theoretical stresses  $\sigma_x$  of Figs. 2 through 7 appear to differ from the test results by a translation, i.e., the theoretical stresses  $\sigma_x$  are too low at the major axis and too high at the minor axis. This effect is graphically illustrated in Figs. 9 through 11 in which the stresses  $\sigma_x$  have been separated into membrane and bending components,  $(\sigma_x)_{\text{membrane}} = (1/2)[(\sigma_x)_{\text{inner}} + (\sigma_x)_{\text{outer}}]$  and  $(\sigma_x)_{\text{bending}} = (1/2)[(\sigma_x)_{\text{inner}} - (\sigma_x)_{\text{outer}}]$ . Here it is seen that the theoretical values for  $(\sigma_x)_{\text{bending}}$  agree well with the test data, showing that the discrepancy between theory and test stresses  $\sigma_x$  is due to erroneous theoretical values

for  $(\sigma_x)_{\text{membrane}}$  alone.

In this connection the following considerations indicate that the above solution, based upon using the local skin thicknesses of Fig. 1, can not be expected to yield accurate results for the stresses  $(\sigma_x)_{\text{membrane}}$ . When the two different local skin thicknesses of Fig. 1 are used in solutions for oval shells of uniform thickness subjected to a hydrostatic pressure two different axial contractions are obtained. The thinner shell contracts more than the thicker shell. In the tests of the shell of Fig. 1, however, the axial contraction was the same for both the thin and thick portions. If the thin and thick shells (in which the local thickness has been used) were considered as simple one-dimensional bars and forced to have the same axial contraction without changing the net end load, the thinner shell would have to be stretched, and the thick shell compressed. This would increase the axial membrane stress in the thin shell and decrease the corresponding stress in the thick shell, i.e., such a correction would shift the theoretical curves for  $\sigma_x$  towards the test data. However, using this simple one-dimensional procedure, in which the cross-sectional areas of the bars are assumed to be given by the cross-sectional areas of the thin and thick portions of the shell (Fig. 1), results in a correction to  $(\sigma_x)_{\text{membrane}}$  of +5.8 for  $0 \text{ (major axis)} \leq \theta \leq 62.1^\circ$

8.

and  $-2.6$  for  $62.1^\circ \leq \theta \leq 90^\circ$  (minor axis). The correction can therefore only be considered as qualitative, since the magnitudes are only about  $1/4$  of those required (see Figs. 9 through 11, for example).

## REFERENCES

1. Couch, W.P. and Pulos, J.G.: Progress Report--Experimental Stresses and Strains in a Ring-Stiffened Cylinder of Oval Cross-Section (Major-to-Minor Axis Ratio of 1.5). David Taylor Model Basin, Report 1726, March 1963.
2. Vafakos, W.P., Romano, F. and Kempner, J.: Clamped Short Oval Cylindrical Shells under Hydrostatic Pressure. J. Aerospace Sciences, Vol. 29, No. 11, Nov. 1962. (Also, PIBAL Report No. 594, Polytechnic Institute of Brooklyn, June 1961).
3. Vafakos, W.P., Nissel, N. and Kempner, J.: Energy Solution for Simply Supported Short Oval Shells. PIBAL Report No. 667, Polytechnic Institute of Brooklyn, August 1963.

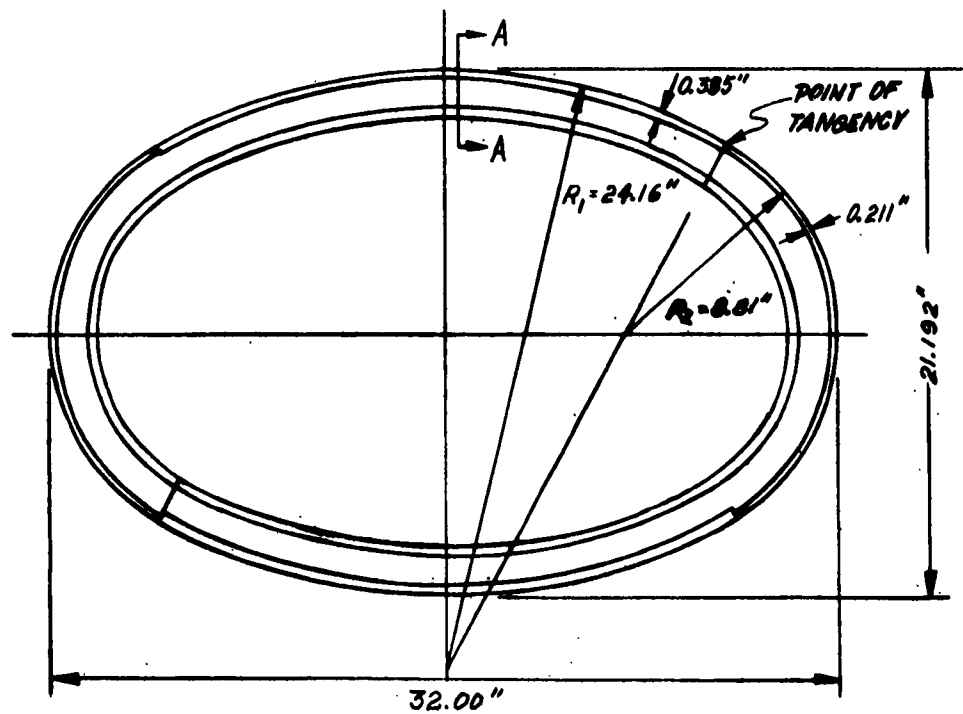
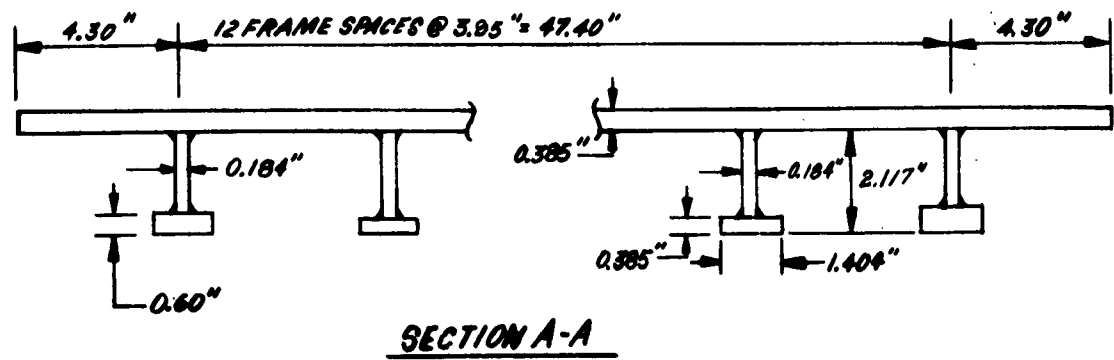


Figure 1 - Details of Model EC-1  
(Reproduced from Ref. 1)

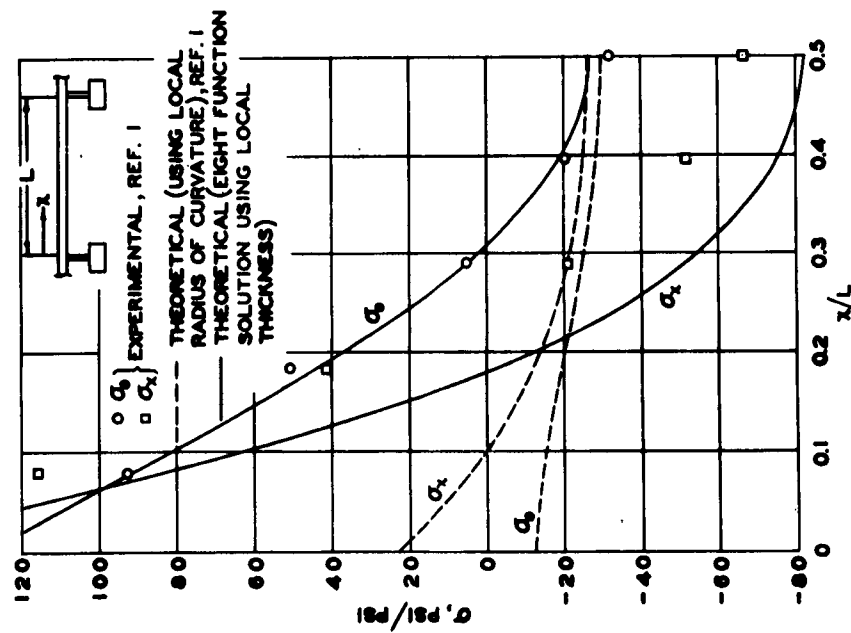


FIG. 2 STRESS DISTRIBUTION ON OUTSIDE SURFACE OF THE SHELL AT THE MAJOR AXIS

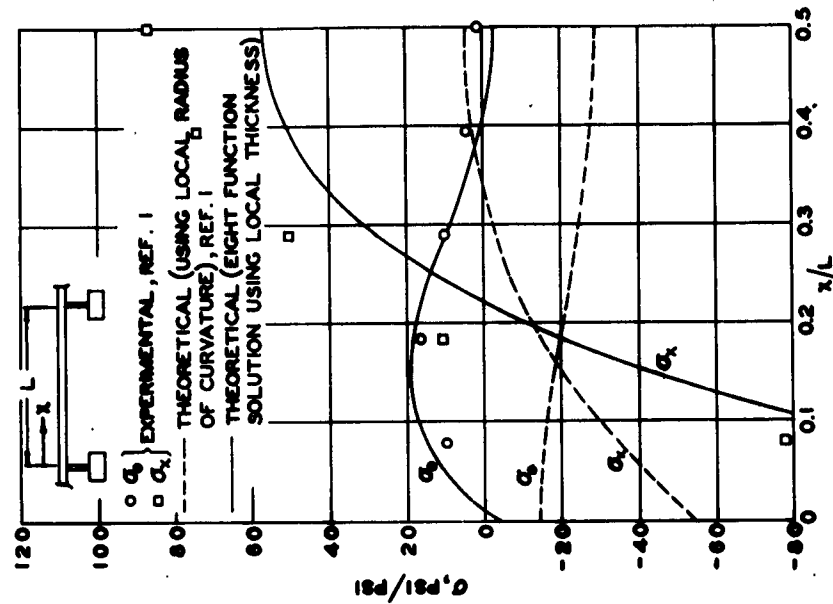


FIG. 3 STRESS DISTRIBUTION ON INSIDE SURFACE OF THE SHELL AT THE MAJOR AXIS



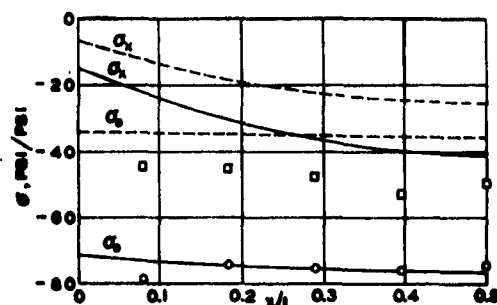
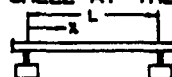


FIG. 4 STRESS DISTRIBUTION ON OUTSIDE SURFACE OF THE SHELL AT THE MINOR AXIS



- $\sigma_x$
- $\sigma_y$
- △  $\sigma_z$
- ◇  $\sigma_\theta$
- EXPERIMENTAL, REF. 1
- THEORETICAL (USING LOCAL RADIUS OF CURVATURE), REF. 1
- THEORETICAL (EIGHT FUNCTION SOLUTION USING LOCAL THICKNESS)

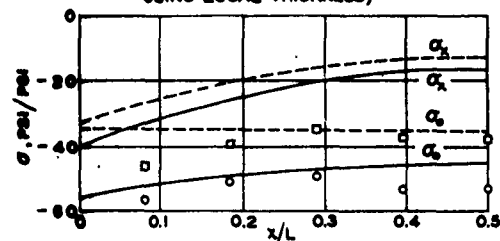


FIG. 5 STRESS DISTRIBUTION ON INSIDE SURFACE OF THE SHELL AT THE MINOR AXIS

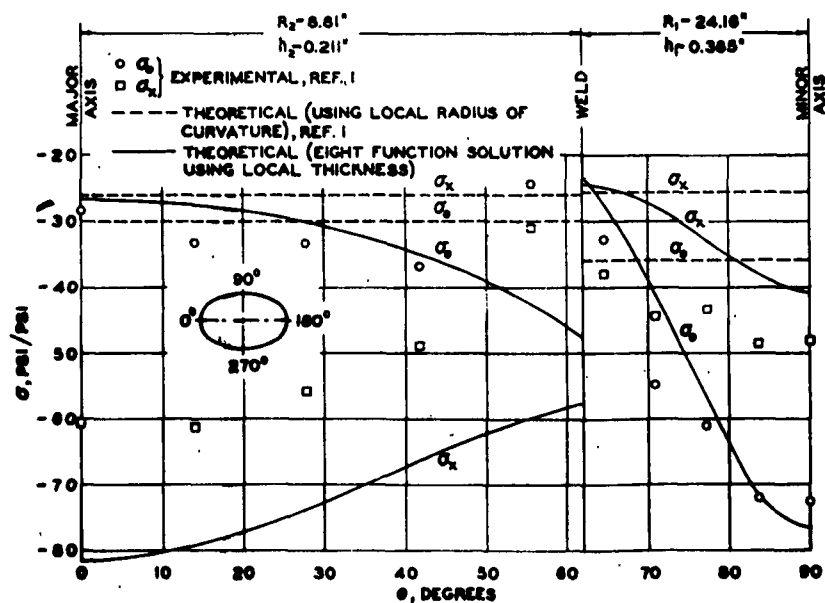


FIG. 6 MID-BAY STRESS DISTRIBUTION ON OUTSIDE SURFACE OF A QUADRANT OF SHELL

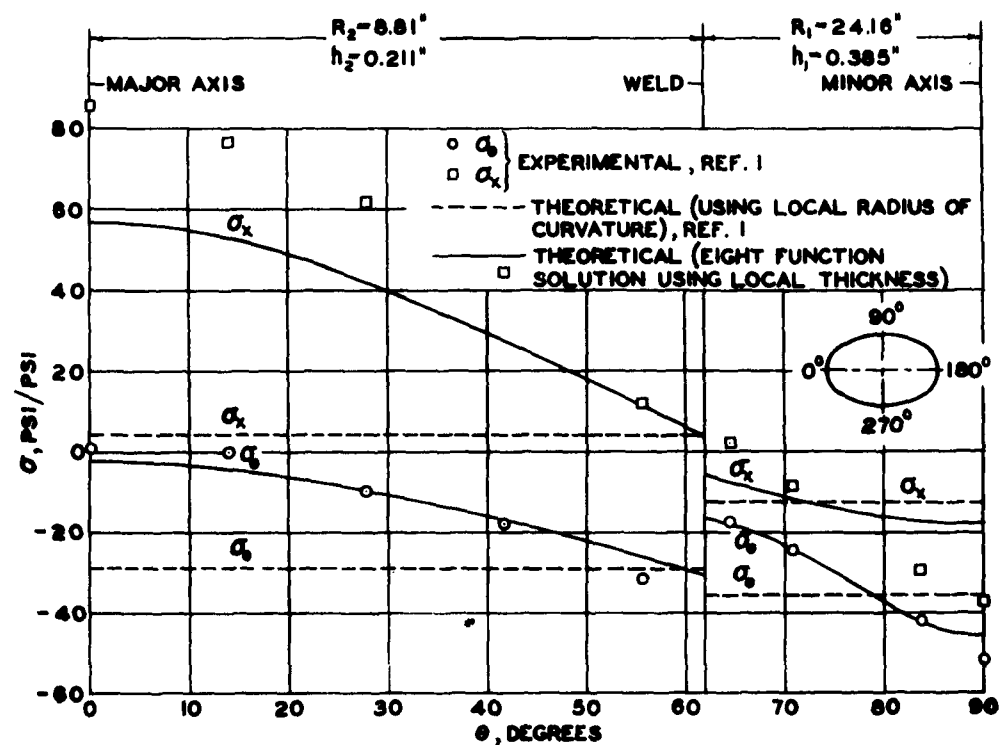


FIG. 7 MID-BAY STRESS DISTRIBUTION ON INSIDE SURFACE OF A QUADRANT OF SHELL

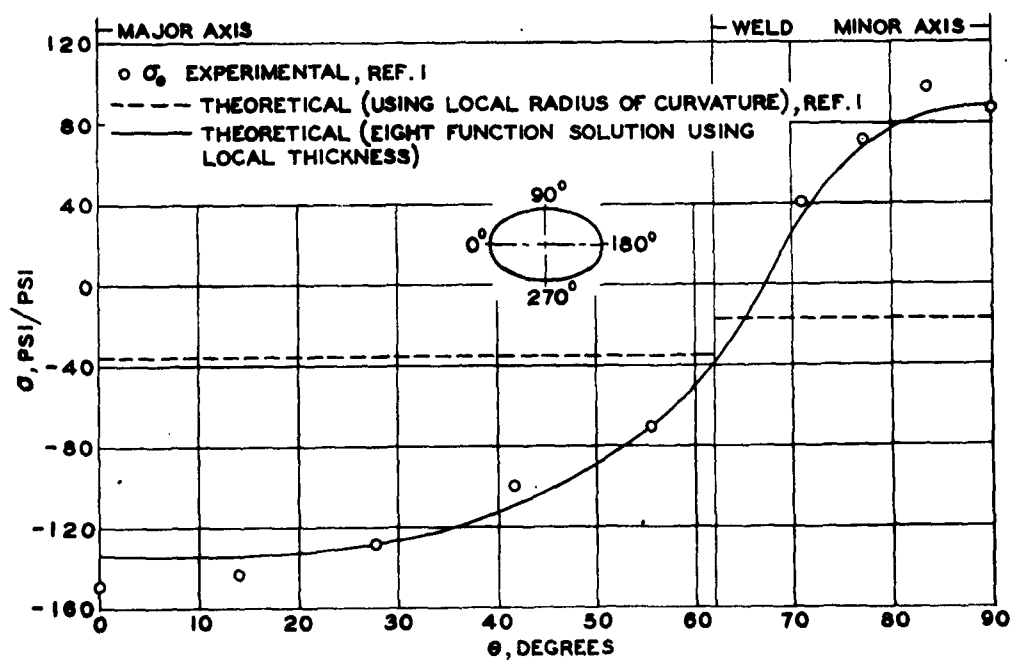


FIG. 8 CIRCUMFERENTIAL FLANGE STRESS FOR A QUADRANT OF FRAME

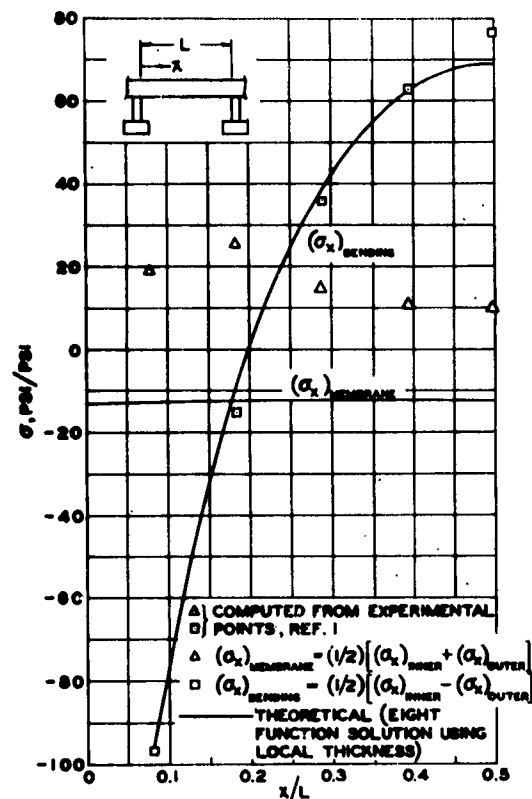


FIG. 9 AXIAL MEMBRANE AND BENDING STRESSES AT THE MAJOR AXIS

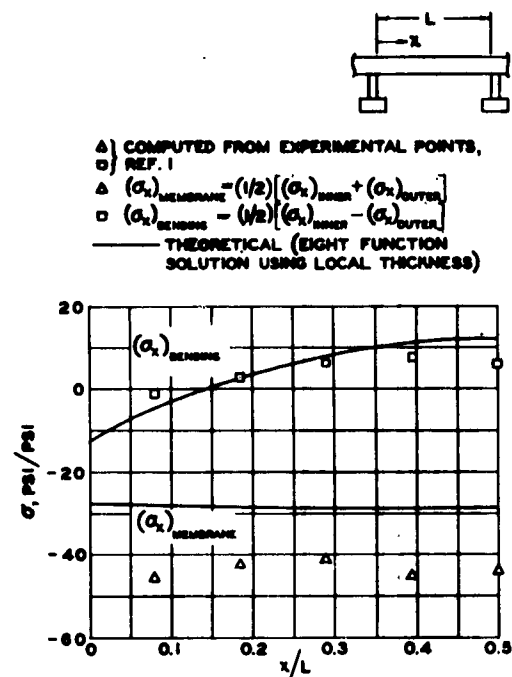


FIG. 10 AXIAL MEMBRANE AND BENDING STRESSES AT THE MINOR AXIS

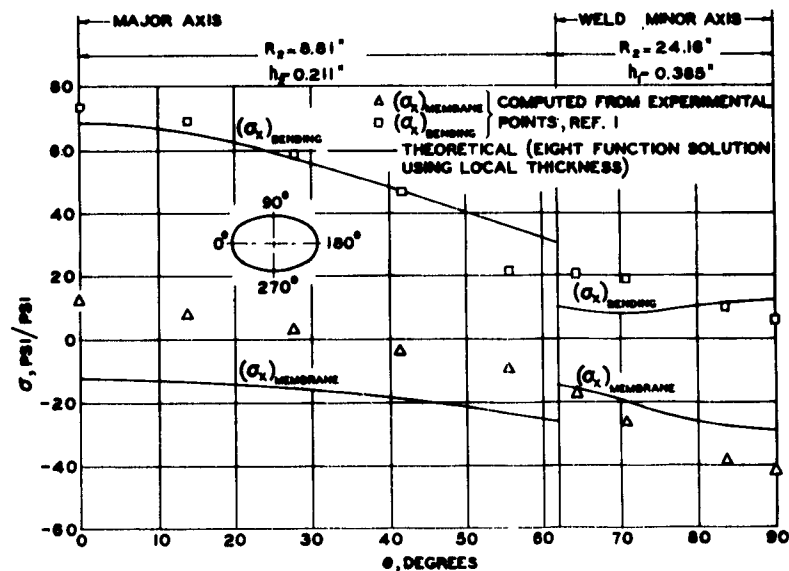


FIG. 11 AXIAL MEMBRANE AND BENDING STRESSES AT MID-BAY FOR A QUADRANT OF SHELL

Distribution List for  
Unclassified  
Technical and Final Reports Issued Under  
Office of Naval Research - Contract Nonr 839(14)

I. Administrative, Reference and Liaison Activities of ONR

Chief of Naval Research	Director	
Department of the Navy	Office of Naval Research	
Washington 25, D.C.	Branch Office	
Attn: Code 432	207 West 24 Street	(1)
Code 438	New York 11, N.Y.	(2)
Code 439		(1)
Director, Naval Research Lab.	Commanding Officer	
Washington 25, D.C.	Office of Naval Research	
Attn: Tech. Info. Officer	Navy #100 Fleet P.O.	(25)
Technical Library	New York, New York	
Mechanics Division	Armed Services Tech. Info. Agcy.	
	Document Service Center	
	Arlington Hall Station	
	Arlington 12, Virginia	(10)

II. Department of Defense and Other Interested Government Activities

(A) General

Research and Devel. Bd.	Engineering Res. & Dev. Lab.	
Dep't of Defense	Fort Belvoir, Virginia	
Pentagon Building	Attn: Structures Br.	(1)
Washington 25, D.C.		
Attn: Library Code 3D-1075	Off. of the Chief of Eng.	(1)
Chief	Asst. Chief for Military Const.	
Defense Atomic Support Agcy	Dept. of the Army	
Washington 25, D.C.	Bldg. T-7, Gravelly Point	
Attn: Document Library Br.	Wash. 25, D.C.	
	Attn: Struct. Br. (ENGEA)	(1)

(B) Army

Chief of Staff	Off. of the Chief of Engrs.	
Dep't of the Army	Asst. Chief for Military Operations	
Research & Devel. Div.	Dept. of the Army	
Washington 25, D.C.	Bldg. T-7, Gravelly Point	
Attn: Chief of Res. & Dev.	Wash. 25, D.C.	
	Attn: Structures Devel. Br.	
	(W. Woollard)	(1)
Office of the Chief of Engrs.	U.S. Army Waterways Exp. Sta.	
Asst. Chief for Works	P.O. Box 631	
Dept. of the Army	Halls Ferry Road	
Bldg. T-7, Gravelly Point	Vicksburg, Mississippi	
Washington 25, D.C.	Attn: Col. H.J. Skidmore	(1)
Attn: Structural Br.		
(R.L. Bloor)		

Distribution List (Cont.) - Unclassified

The Commanding General Sandia Base P.O. Box 5100 Albuquerque, New Mexico Attn: Col. Canterbury (1)	Commanding Officer Underwater Explosion Res. Div. Norfolk Naval Shipyard Portsmouth, Virginia Attn: Code 290 (1)
Office of the Chief of Ordnance Office of Ordnance Research Dept. of the Army The Pentagon Annex #2 Washington 25, D.C. Attn: ORDTB-PS (1)	Commander Portsmouth Naval Shipyard Portsmouth, N.H. Attn: Design Div. (1)
Ballistics Research Lab. Aberdeen Proving Ground Aberdeen, Maryland Attn: Dr. C.W. Lampson (1)	Director Materials Laboratory New York Naval Shipyard Brooklyn 1, N.Y. (1)
(C) <u>NAVY</u>	Naval Ordnance Lab. White Oak, Maryland RFD 1, Silver Spring, Md. Attn: Mechanics Div. (1) Explosive Div. (1) Mech. Eval. Div. (1)
Chief of Naval Operations Dept. of the Navy Washington 25, D.C. Attn: OP-31 (1) OP-363 (1)	Commander U.S. Naval Ordnance Test Sta. Inyokern, Calif. Post Office China Lake, Calif. Attn: Scientific Officer (1)
Chief of Bureau of Ordnance Dept. of the Navy Washington 25, D.C. Attn: Ad-3, Technical Lib. (1) Rec., P.H. Girouard (1)	Naval Ordnance Test Sta. Underwater Ordnance Div. Pasadena, California Attn: Structures Div. (1)
Chief, Bureau of Ships Dept. of the Navy Washington 25, D.C. Attn: Director of Research (2) Code 423 (1) Code 442 (1) Code 421 (1)	Chief of Bureau of Aeron. Dept. of the Navy Washington 25, D.C. Attn: TD-41 Technical Library (1)
Commanding Officer and Dir. David Taylor Model Basin Washington 7, D.C. Attn: Code 140 (1) Code 600 (1) Code 700 (3) Code 720 (1) Code 725 (1) Code 731 (1) Code 740 (2)	Chief, Bureau of Yards & Docks Dept. of the Navy Washington 25, D.C. Attn: Code P-314 (1) Code C-313 (1)

Distribution List (Cont) - Unclassified

Officer in Charge Naval Civil Engrg. Res. & Evaluation Lab. Naval Station Port Hueneme, Calif.	(1)	Flight Research Lab. Wright-Patterson Air Force Base Dayton, Ohio Attn: Chief, Applied Mechs. Group	(1)
Superintendent U.S. Naval Postgraduate School Annapolis, Maryland	(1)	<u>(E) OTHER GOV'T AGENCIES</u>	
<u>(D) AIR FORCE</u> Commanding General U.S. Air Force The Pentagon Washington 25, D.C. Attn: Res. & Devel. Div.	(1)	U.S. Atomic Energy Comm. Division of Research Washington, D.C.	(1)
Deputy, Chief of Staff Operations Air Targets Division Headquarters, U.S. Air Force Washington 25, D.C. Attn: AFOIN-T/PV	(1)	Director National Bureau of Standards Washington, D.C. Attn: Dr. W.H. Ramberg	(1)

Supplementary Distribution List

Professor Lynn Beedle Fritz Engineering Laboratory Lehigh University Bethlehem, Pennsylvania	(1)	Professor B.A. Boley Dept. of Civil Engineering Columbia University Broadway at 117th St. New York 27, N.Y.	(1)
Professor R.L. Bisplinghoff Dept. of Aeronautical Engrg. Massachusetts Inst. of Tech. Cambridge 39, Mass.		Professor P. Chiarulli Technology Center Illinois Inst. of Tech. Chicago 16, Illinois	(1)
Professor Hans Bleich Dept. of Civil Engineering Columbia University Broadway at 117th St. New York 27, N.Y.		Professor R.J. Dolan Dept. of Theo. & Appl. Mechs. University of Illinois Urbana, Illinois	(1)

Distribution List (Cont) - Unclassified

Mr. Martin Goland Southwest Research Institute 8500 Culebra Road San Antonio 6, Texas	(1)	Professor L.S. Jacobsen Dept. of Mechanical Engrg. Stanford University Stanford, California	(1)
Dr. J.N. Goodier School of Engineering Stanford University Stanford, California	(1)	Professor J. Kempner Dept. of Aerospace Engrg. & Applied Mechanics Polytechnic Institute of Brooklyn 333 Jay Street Brooklyn 1, New York	(1)
Professor R.M. Hermes College of Engineering University of Santa Clara Santa Clara, California	(1)	Professor George Lee Dept. of Aero. Engrg. Rensselaer Polytechnic Inst. Troy, New York	(1)
Professor R.J. Hansen Dept. of Civil & Sanitary Eng. Mass. Inst. of Technology Cambridge 39, Mass.	(1)	Professor Glen Murphy Dept. of Theo. & Appl. Mechs. Iowa State College Ames, Iowa	(1)
Professor M. Hetenyi Stanford University Dept. of Eng. Mechs. Stanford, California	(1)	Professor Wm. A. Nash University of Florida Gainesville, Florida	(1)
Dr. N.J. Hoff, Head Division of Aeron. Engrg. Stanford University Stanford, California	(1)	Professor N.M. Newmark Dept. of Civil Engrg. University of Illinois Urbana, Illinois	(1)
Dr. Bernard Shaffer Dept. of Mechanical Eng. New York University University Heights New York 53, New York	(1)	Prof. Jesse Ormondroyd University of Michigan Ann Arbor, Michigan	(1)
Dr. J.H. Hollomon General Electric Res. Labs. 1 River Road Schenectady, New York	(1)	Prof. Eugene J. Brunella, Jr. Dept. of Aeron. Engrg. Princeton University Princeton, New Jersey	(1)
Dept. of Applied Mechanics Johns Hopkins University Baltimore 18, Maryland	(1)	Dr. D.O. Brush Structures Dept. 53-13 Lockheed Aircraft Corp. Missile Systems Division Sunnyvale, California	(1)

Distribution List (Cont) - Unclassified

Professor Aris Phillips Winchester Hall 15 Prospect Street Yale University New Haven, Connecticut	(1)	Professor J.E. Cermak Dept. of Civil Engineering Colorado State University Fort Collins, Colorado	(1)
Dr. W. Prager, Chairman Graduate Div. of App. Math. Brown University Providence 12, Rhode Island	(1)	Professor E. Sternberg Division of Applied Math. Brown University Providence 12, Rhode Island	(1)
Professor E. Reissner Dept. of Mathematics Mass. Inst. of Tech. Cambridge, Mass.	(1)	Professor F.K. Teichman Dept. of Aeron. Engrg. New York University University Heights Bronx, New York	(1)
Mr. M.A. Sadowski Dept. of Mechanics Rensselaer Polytechnic Inst. Troy, New York	(1)	Professor A.C. Eringen Dept. of Aeron. Engrg. Purdue University Lafayette, Indiana	(1)
Dr. James Sheng c/o Dynamic Sciences Dept. 41-191-015 Space & Info. Sys. Div. 12214 Lakewood Blvd. Downey, Calif.	(1)	Professor Paul Lieber Geology Dept. University of California Berkeley 4, California	(1)
Professor Nicholas Perrone Office of Naval Research Washington 25, D.C. Attn: Code 438	(1)	Mr. K.H. Koopman, Secretary Welding Res. Council of the Engrg. Foundation 345 East 47th Street New York 17, New York	(2)
Professor J.E. Stallmeyer Talbot Laboratory Dept. of Civil Engineering University of Illinois Urbana, Illinois	(1)	Professor Walter T. Daniels School of Engrg. and Architecture Howard University Washington 1, D.C.	(1)
Commanding Officer USNNOEU Kirtland Air Force Base Albuquerque, New Mexico Attn: Code 20 (Dr. J.N. Brennan)	(1)	Commander Wright Air Development Center Wright-Patterson Air Force Base Dayton, Ohio Attn: Dynamics Branch	(1)



Distribution List (Cont) - Unclassified

Commander

WADD

Wright-Patterson Air Force Base

Ohio

Attn: WWRC (1)

WWRMDS (1)

WWRMDD (1)

Professor W.J. Hall

Department of Civil Engrg.

University of Illinois

Urbana, Illinois (1)

Professor R.P. Harrington, Head

Dept. of Aero. Engineering

University of Cincinnati

Cincinnati 21, Ohio (1)